General Disclaimer

One or more of the Following Statements may affect this Document

- This document has been reproduced from the best copy furnished by the organizational source. It is being released in the interest of making available as much information as possible.

- This document may contain data, which exceeds the sheet parameters. It was furnished in this condition by the organizational source and is the best copy available.

- This document may contain tone-on-tone or color graphs, charts and/or pictures, which have been reproduced in black and white.

- This document is paginated as submitted by the original source.

- Portions of this document are not fully legible due to the historical nature of some of the material. However, it is the best reproduction available from the original submission.

NASA Technical Memorandum 78541

An Examination of a Group-Velocity Criterion for the Breakdown of an Idealized Vortex Flow

Chon-Yin Tsai and Sheila E. Widnail

June 1979

National Aeronautics and
Space Administration

NOMENCLATURE

a	speed of sound
C_g	group velocity of wave propagation in axial direction; $-d\omega/dk$
C_p	phase velocity of wave propagation in axial direction; $-\omega/k$
H	total head function
k	axial wave number
n	azimuthal wave number
P	pressure of basic flow field
$\tilde{p}$	pressure of disturbance flow field
$\mathscr{P}$	amplitude function of pressure disturbance
q	ratio of swirl velocity to axial velocity at inlet of divergent duct
(r,θ,z)	cylindrical coordinates at inlet of duct; r and z are normalized by R_i
(r^*,θ^*,z^*)	local cylindrical coordinates; $r^* = r/R(z_s)$, $\theta^* = \theta$, $z^* = z - z_s$
R_i	radius at duct inlet
$R(z)$	geometric shape of duct normalized by R_i
(U,V,W)	velocities of basic flow field; U in radial direction, W in axial direction
$(\tilde{u},\tilde{v},\tilde{w})$	velocities of disturbance flow field; $\tilde{u}$ in radial direction, $\tilde{w}$ in axial direction
$(\mathscr{U},\mathscr{V},\mathscr{W})$	amplitude functions of velocity disturbances; $\mathscr{U}$ in radial direction, $\mathscr{W}$ in axial direction
W_i	uniform axial velocity at inlet of divergent duct
ψ	stream function of basic flow field
Γ	circulation function
Ω	constant angular velocity

PRECEDING PAGE BLANK NOT FILMED

ω	frequency of disturbance
ρ	water density

Subscripts

c	critical state
i	function evaluated at inlet of divergent duct, z = 0
o	function evaluated at r = 0
s	axial station

AN EXAMINATION OF A GROUP-VELOCITY CRITERION FOR THE BREAKDOWN OF AN IDEALIZED VORTEX FLOW

Chon-Yin Tsai*

Ames Research Center

and

Sheila E. Widnall**

Massachusetts Institute of Technology

SUMMARY

The phenomenon of vortex breakdown is believed to be associated with a finite-amplitude wave that has become trapped at the critical or breakdown location. The conditions at which the propagating waves become trapped at a certain axial location is examined here by use of a group-velocity criterion implied by Landahl's general theory of wave trapping. Contrary to previous theories, the present explanation may cover both axisymmetric and asymmetric breakdown. In order to investigate the relationship between wave trapping and vortex breakdown, a numerical study is made here of an ideal vortex having constant vorticity and uniform axial velocity at the inlet of a slowly diverging duct. The solution presented by Batchelor for the flow field of a vortex flow in a slowly varying duct is well known. The linear wave propagation analysis is then applied to this base flow at several axial stations for several values of the ratio of swirl velocity to axial velocity at the inlet of the divergent duct, assuming a locally parallel flow. The dispersion relations and hence the group velocities of both the symmetric ($n = 0$) and asymmetric modes ($n = \pm 1$) are investigated. The existence of a critical state in the flow (at which the group velocity vanishes), and its relationship to the stagnation point on the axis of the duct and to the occurrence of an irregular singularity in the equations governing wave propagation in the flow field are discussed.

INTRODUCTION

The study of the stability of vortex flows is important in many fields, such as aeronautics, combustion, and geophysics. One of the instability

---

*National Research Council Research Associate. Ames Research Center, NASA, Moffett Field, California 94035; currently at Boeing Commercial Airplane Company, Seattle, Washington.

**Professor, Department of Aeronautics and Astronautics, Massachusetts Institute of Technology, Cambridge, Massachusetts 02139.

mechanisms of vortex flows is the so-called vortex breakdown or vortex bursting. That is, the breakdown of vortex motion is identified as occurring when the swirl and axial flow undergo an abrupt and drastic structure change along the axis of the vortex. The breakdown or burst is often characterized by the formation of an internal stagnation point on the vortex axis (ref. 1), followed by a reversed flow in a region of limited axial extent. The first documented vortex breakdown phenomenon was reported by Peckham and Atkinson (unpublished report, 1957) in an investigation of the aerodynamics of delta wings. Vortex breakdown also has been observed in the swirling flows through nozzles and diffusers. Practical applications of the vortex breakdown phenomenon occur in two ways. In some cases, one wishes to avoid or delay the occurrence of vortex breakdown, as in the flow over a delta wing, to control stall. In other cases, one wishes to induce vortex breakdown to dissipate strong velocity gradients in the trailing vortices behind large aircraft during takeoff and landing to reduce the hazard to following aircraft or to reduce blade/vortex interaction noise of helicopter rotors. Solutions to these problems require an improved understanding of the vortex breakdown phenomenon. It is important to know which vortices will suffer breakdown and what are the major features of the recirculation zone and of the downstream flow field.

In order to isolate the phenomenon under more controlled circumstances, experiments on vortices are usually performed in ducts. Harvey (ref. 2) used a cylindrical vortex formed in a long duct of constant cross section to study vortex breakdown. By varying the amount of swirl imparted to the fluid before it entered the duct, he found that the breakdown was the intermediate stage between two basic types of rotating flows. He concluded that breakdown is a characteristic of "critical" phenomenon and that it is not a hydrodynamic instability. Sarpkaya (ref. 3) obtained breakdown in a divergent duct with less swirl than that required in a duct of constant cross section. He observed three types of vortex breakdown: double helix (mild), spiral (followed by turbulent mixing), and axisymmetric (followed by a thicker vortex core, then a spiral breakdown, and, finally, by turbulent mixing). Faler and Lebovich (ref. 4) conducted experiments in an apparatus modeled after Sarpkaya's and, from their flow visualization studies, found three additional states of vortex disruption. Their experimental results show that the type and location of breakdown were dependent on the Reynolds number and circulation distribution of the flow. The first detailed velocity measurements of the vortex flow field containing breakdown in a slightly diverging duct were obtained by using a laser Doppler anemometry (refs. 4-6). Although theoretical attempts to explain the vortex breakdown phenomenon are numerous, none have led to a satisfactory understanding of the observed flow. The various theories for vortex breakdown have been reviewed and classified into three categories by Hall (ref. 7) and Lebovich (ref. 1): (a) vortex breakdown is proposed to be the consequence of hydrodynamic instability, (b) vortex breakdown is analogous to the separation of a boundary layer in an adverse pressure gradient, and (c) vortex breakdown is the result of some type of critical condition existing in the flow. Theories using hydrodynamic instability as the sole mechanism for vortex breakdown are no longer considered satisfactory (e.g., Ludwieg's theory (ref. 8) is mathematically inconsistent if applied to duct flow (see review by Lebovich (ref. 1)). The analogy between vortex breakdown and the separation of a boundary layer does not suggest any physical mechanism for the

phenomenon and is incomplete because of the restriction to axisymmetric flow. The idea of a critical condition existing in a vortex flow was introduced by Squire (ref. 9). Based on phase speeds, Squire proposed that if infinitesimal amplitude axisymmetric waves have zero phase speed, then the disturbances originating downstream may propagate upstream and cause breakdown. Although Squire's explanation of vortex breakdown has some weaknesses, his idea of the possible appearance of infinitesimal standing waves in the flow has led to the development of various wave theories for vortex breakdown. Benjamin (ref. 10) considered vortex breakdown as precisely analogous to the hydraulic jump in open channel flow. That is, the frictionless swirling flows generally occur in conjugate pairs wherein both can form parts of the same overall system. For a given distribution of total head and circulation over the stream surfaces, one possible state of flow is defined as "subcritical" — an infinitesimal axisymmetric standing wave can occur. Its conjugate state is defined as "supercritical" — no standing wave is possible. The analytical condition for the existence of infinitely long, axisymmetric standing waves, $C_p = 0$, has a fundamental role in Benjamin's theory.

Randall and Lebovich (ref. 11) developed a theory of long, weakly nonlinear waves propagating along critical flows in tubes of variable cross section. Although the structural features of the vortex breakdown predicted by a nonlinear trapped wave model are consistent with many of the experimentally observed features, there are still deficiencies in the theory — reversed swirls predicted in the bubble interior are physically impossible and the spiral form of breakdown is excluded. Numerical experiments with the Navier-Stokes equations restricted to axial symmetry and steady flow throughout the entire flow field, including the breakdown region, have been studied by several investigators. Although there are some qualitative points of agreement between physical and numerical experiments, there are a number of ways in which the numerical and physical experiment are quite different (see ref. 1). The most common deficiencies in previous theories are that the spiral form of breakdown is excluded and the recirculation zone itself is assumed to be axisymmetric. Therefore, a different approach to the study of vortex breakdown is required.

Using Landahl's (ref. 12) general theory of wave focussing as the framework for analysis, Bilanin (ref. 13) suggested and explored the possibility that vortex breakdown is associated with a trapped finite-amplitude wave. He defined the vortex flow as "supercritical" or "subcritical" when the group velocity of infinitesimal waves is in the "downstream" or in "both" directions along the axis of the vortex. Thus, the same flow may be subcritical to axisymmetric waves and supercritical to spiral wave modes. He then obtained the critical state (defined as occurring when $C_g = 0$) for the propagation of various wave types along a line vortex undergoing solid body rotation with uniform axial velocity. By ranking the modes according to their ability to signal upstream, he postulated which type of breakdown (axisymmetric vs. spiral) would first occur.

In the present study, the linear wave trapping process is explored for an ideal model of vortex flow — for example, a vortex having constant vorticity Ω and constant axial velocity W_i at the inlet of a slowly diverging duct.

This flow model has the simplest entry conditions and provides a hypothetical configuration that has a minimum number of variable parameters. Although this flow is not a good model of vortex breakdown because it has negative swirls downstream of the stagnation point, the wave characteristics of these profiles may be of some interest.

In the following, we first discuss the group-velocity criterion for vortex breakdown as derived from Landahl's (ref. 12) general wave trapping theory. Then, the linear wave propagation analysis is formulated and applied to the idealized model of vortex flow in a slightly diverging duct obtained in analytic form by means of the inviscid quasi-cylindrical approximation. The dispersion relations and hence the group velocities are then calculated numerically.

Dr. Vernon J. Rossow suggested the application of wave trapping theory to the theoretical model of uniform rotation and axial velocity. The authors thank Dr. Rossow for valuable discussions and encouragement.

WAVE TRAPPING THEORY AND VORTEX BREAKDOWN

Landahl (ref. 12) developed a general theory for the wave mechanics of breakdown to determine under what conditions the steady or unsteady laminar flow will break down into high-frequency oscillations. The analysis of a small-scale secondary wave riding on a large-scale inhomogeneity reveals that the breakdown mechanism occurs when the group velocity of a self-excited secondary wave is near the phase velocity of the primary wave. To illustrate, a simple example of wave trapping given by Landahl is included here. Consider the supersonic one-dimensional gas flow in a Laval nozzle. An oscillating disturbance produces two sets of acoustic waves: an advancing wave with a propagation velocity $W + a$ (where W and a are the local flow and sound velocity, respectively) and a receding wave with a propagation velocity $W - a$. Linear theory predicts the amplitude of the receding wave as $(W - a)^{-1/2}$. Therefore, if sonic flow exists at the throat, the amplitude of the waves would become large and could be predicted only by a nonlinear analysis. The singularity in the linear theory is a result of a concentration of wave energy produced by consecutive wave fronts catching up with each other. The wave trapping process is a possibility for any inhomogeneous continuum system which can support propagating waves that are small relative to the scale of inhomogeneities. The large-scale inhomogeneity could be produced by a primary wave, by viscous dissipation, or by changes in the boundaries of the flow field. In the present study, the inhomogeneity is assumed to be induced by the slowly diverging wall of the duct. Landahl's breakdown criterion for steady vortex flow in a duct requires that the group velocity, C_g, of infinitesimal waves be zero at some point. The vortex flow may then be classified as "supercritical" to a wave type when the group velocity of that wave propagates in the downstream direction ($C_g > 0$), and "subcritical" if the wave can propagate in either direction. The dispersion relations and hence the group velocities are obtained by solving the eigenvalue problem at each axial station as if the flow were locally parallel. The location where the group velocity of wave

disturbance is zero is proposed as the place where wave trapping and therefore the breakdown of vortex flow would occur. Typically, only one type of wave mode (axisymmetric or spiral) would be critical at any station in the flow.

FORMULATION OF THE PROBLEM

It was proposed in the previous section that the phenomenon of vortex breakdown is associated with the trapping of finite-amplitude waves propagating along the vortex. To investigate the relationship between wave structure, wave trapping, and vortex breakdown, we consider a slowly varying basic flow field perturbed by axisymmetric and asymmetric disturbance waves. The problem is formulated in the following two sections.

Basic Flow Field

In the present study, the basic flow field is taken as a swirling flow inside a duct with a small divergent angle. Using cylindrical polar coordinates (r,θ,z) with the corresponding velocity components (U,V,W) and introducing the stream function $\psi(r,z)$ such that $U = (-1/r)(\partial\psi/\partial z)$ and $W = (1/r)(\partial\psi/\partial r)$, the inviscid, incompressible equations of motion can be reduced to (ref. 14)

$$\frac{\partial^2\psi}{\partial z^2} + \frac{\partial^2\psi}{\partial r^2} - \frac{1}{r}\frac{\partial\psi}{\partial r} = r^2\frac{dH}{d\psi} - \Gamma\frac{d\Gamma}{d\psi} \tag{1}$$

where

$$H(\psi) = \frac{1}{2}(U^2 + V^2 + W^2) + \frac{P}{\rho} \qquad \text{(Total head function)}$$

$$\Gamma(\psi) = rV \qquad \text{(Circulation)}$$

The pressure P is calculated from the radial equation of motion.

For the relatively simple case considered here, the fluid at the inlet of the divergent duct has uniform axial velocity W_i and rotates as a rigid body with angular velocity Ω; the entrance conditions are therefore given by

$$\psi = \frac{W_i}{2} r_i^2$$

$$\Gamma = \Omega r_i^2 = \frac{2\Omega}{W_i}\psi$$

and

$$\frac{dH}{d\psi} = \frac{2\Omega^2}{W_i} + \frac{1}{r_i^2}\frac{\partial^2\psi}{\partial_z^2} = \frac{2\Omega^2}{W_i} + \frac{W_i}{2\psi}\frac{\partial^2\psi}{\partial_z^2}$$

where the subscript i of r_i denotes the radial coordinate at the inlet of the divergent duct. The dependence of H and Γ on ψ must hold throughout the flow field. The governing equation (1) then takes the form

$$\frac{\partial^2\psi}{\partial z^2} + \frac{\partial^2\psi}{\partial r^2} - \frac{1}{r}\frac{\partial\psi}{\partial r} = \frac{2\Omega^2}{W_i}r^2 - \frac{4\Omega^2}{W_i^2}\psi + W_i\frac{r^2}{2\psi}\frac{\partial^2\psi}{\partial z^2} \tag{2}$$

For the flow in a slowly diverging duct, the quasi-cylindrical approximation is applicable because the variations in axial direction are much smaller than variations in the radial direction. Therefore, equation (2), in dimensionless form with length scale R_i (radius at the duct inlet) and velocity scale W_i, becomes

$$\frac{\partial^2\psi}{\partial r^2} - \frac{1}{r}\frac{\partial\psi}{\partial r} = 2q^2r^2 - 4q^2\psi$$

The boundary conditions are

$$\psi(0) = 0$$

$$\psi(R) = \frac{1}{2}$$

where R is the dimensionless local radius of the linearly divergent duct and

$$q = \frac{R_i\Omega}{W_i}$$

The stream function for the flow field is written in analytic form as (ref. 7):

$$\psi = \frac{1}{2}r^2 + \frac{1}{2}F(R)rJ_1(2qr) \tag{3}$$

with

$$F(R) = \frac{1 - R^2}{RJ_1(2qR)}$$

where J_1 is the Bessel function of the first kind, of order 1. The quasi-cylindrical solution (3) fails whenever $J_1(2qR) = 0$. This failure of the quasi-cylindrical approximation has often been taken as coincident with the occurrence of vortex breakdown. It will be seen from the results obtained in the next section that C_g (for mode $n = 1$) tends to zero at an axial location much earlier than the location where the quasi-cylindrical approximation fails.

From the stream function, the axial and swirl velocities can be calculated and written as:

$$V = 2q\frac{\psi}{r} = q[r + F(R)J_1(2qr)] \tag{4}$$

$$W = \frac{1}{r}\frac{\partial \psi}{\partial r} = 1 + qF(R)J_o(2qr) \tag{5}$$

where $0 \le r \le R$ and J_o is the Bessel function of the first kind, of order 0. The streamline patterns for various q in a duct of shape function $R(z)$ are given in figures 1 through 5. The z term (normalized by the inlet radius R_i) is the downstream axial coordinate starting at the duct inlet. It can be seen that the reversed swirl velocities occur inside the streamline $\psi = 0$ starting from the stagnation point. Since $\Gamma(\psi)$ is undefined for $\psi < 0$, the solution is meaningless beyond the stagnation point.

Linear Wave Propagation Analysis of a Swirling Flow

The wave propagation analysis of a rotating flow was first studied by Thomson (ref. 15). He investigated the vibration of an isolated column vortex with solid-body rotation surrounded by an irrotational revolving flow and showed that it is stable to all infinitesimal disturbances. Recently, analyses have been made of the stability of flow fields wherein a sheared flow is superimposed on a rotating flow (e.g., refs 16-20). As an application of these analyses, the propagation of an inviscid linear wave along a swirling flow (eqs. (4) and (5)), bounded by a rigid cylindrical duct $0 \le r^* \le 1$ is investigated, where $r^* = r/R$. The coordinates (r^*,θ^*,z^*) for the wave analysis is at each axial station along the duct, assuming that the base flow is locally parallel. This basic flow field is subjected to small perturbations which permits the equations of motion to be linearized. The small perturbations are assumed to be of the form:

$$\{\tilde{u},\ \tilde{v},\ \tilde{w},\ \tilde{p}/\rho\} = \{\mathscr{U}(r^*), \mathscr{V}(r^*), \mathscr{W}(r^*), \mathscr{P}(r^*)\} \exp[i(\omega t + n\theta^* + kz^*)]$$

so that the group velocity is given by

$$C_g = -d\omega/dk$$

and the phase velocity is given by

$$C_p = -\omega/k$$

where $\tilde{u}$, $\tilde{v}$, $\tilde{w}$, and $\tilde{p}$ are the perturbation quantities of radial velocity, tangential velocity, axial velocity, and pressure, respectively. (We drop superscript * in the following analysis for convenience.) The resulting single equation for $\mathscr{U}(r)$ is

$$\frac{d^2\mathscr{U}}{dr^2} + \left(\frac{1}{r} + \frac{1}{S}\frac{dS}{dr}\right)\frac{d\mathscr{U}}{dr} - \left(\frac{\alpha}{\gamma S}\frac{dS}{dr} + \frac{1}{\gamma}\frac{d\alpha}{dr} + \frac{\beta}{\gamma^2 S} - \frac{n\alpha}{\gamma^2}\right)\mathscr{U} = 0 \tag{6}$$

where $\gamma = \omega + nV/r + kW$, k and n are axial and azimuthal wave numbers, $\omega = \omega_r + i\omega_i$ is the complex frequency, and

$$S = \left(k^2 + \frac{n^2}{r^2}\right)^{-1}$$

$$\alpha = \frac{n}{r}\left(\frac{dV}{dr} + \frac{V}{r}\right) + k\frac{dW}{dr} - \frac{\gamma}{r}$$

$$\beta = \gamma^2 - 2\frac{V}{r}\left(\frac{dV}{dr} + \frac{V}{r}\right)$$

$$\eta = -2n\frac{V}{r}$$

The boundary condition at $r = 0$ is

$$\mathscr{U}(0) = \begin{cases} 0 & \text{if } n \neq \pm 1 \\ \text{Finite} & \text{if } n = \pm 1 \end{cases} \tag{7}$$

The boundary condition at the wall, $r = 1$, is

$$\mathscr{U}(1) = 0 \tag{8}$$

Equation (6) along with the boundary conditions (7) and (8) constitute an eigenvalue problem. Instability will result if the imaginary part of the eigenvalue ω is negative for any given pair of wave numbers (n,k).

For the axisymmetric standing wave (i.e., $n = 0$ and $\omega = 0$), which is the case considered by Benjamin (ref. 10), equation (6) is written as

$$\frac{d^2\mathscr{U}}{dr^2} + \frac{1}{r}\frac{d\mathscr{U}}{dr} - \left[\frac{1}{r^2} + \frac{1}{W}\left(\frac{d^2W}{dr^2} - \frac{1}{r}\frac{dW}{dr}\right) - \frac{2V}{rW}\left(\frac{dV}{dr} + \frac{V}{r}\right) + k^2\right]\mathscr{U} = 0 \tag{9}$$

If we substitute the inviscid quasi-cylindrically approximate solution (4) and (5) for the basic flow field, equation (9) can be reduced to the form:

$$\frac{d^2\mathscr{U}}{dr^2} + \frac{1}{r}\frac{d\mathscr{U}}{dr} - \left(\frac{1}{r^2} - 4q^2 + k^2\right)\mathscr{U} = 0 \tag{10}$$

which is independent of the geometry of duct R.

The solution to equation (10), which is well behaved at $r = 0$, is

$$\mathscr{U}(r) = AJ_1[(4q^2 - k^2)^{1/2}r]$$

The boundary condition at $r = 1$ gives

$$k^2 = 4q^2 - b_n^2$$

where $b_n = 0, 3.85, 7.02, \ldots$ are zeros of the Bessel function J_1.

According to Benjamin's (ref. 10) conjugate flow theory, a given state of flow is supercritical if all eigenvalues k^2 are negative, so that no standing wave is possible. The disturbances will then diminish in the upstream direction as $\exp(-kz)$. The state of the flow is considered subcritical if at least the first of k^2 is positive. Therefore, the critical state for the special case considered here occurs when $q_c = b_n/2 = 1.92$. That is, if the ratio q of the vortex flow with solid-body rotation and uniform axial velocity at the inlet of a divergence duct is less than q_c, the flow is supercritical. Since equation (10) is independent of duct geometry, the state of the flow in the whole duct is always supercritical according to the Benjamin's theory and it will not be driven to a subcritical state by the divergence of the wall. This, however, is not the case if the present definition of critical state by the group-velocity criterion is used.

Except for the special case of uniform vorticity and axial flow (inlet condition), the dispersion relation for a general profile must be obtained numerically. Hultgren (ref. 21) presented a numerical method which uses Moulton's method for the stability calculation of rotating gas flows. By use of this method, it was possible to obtain the eigenvalues for the velocity profiles (4) and (5) at each axial station for various q values and determine the group velocity, assuming a locally parallel flow.

Equation (6) has a regular singularity at $r = 0$. A Frobenius power series solution is used to start the numerical integration at the axis of the duct. The solution is then advanced toward the boundary at $r = 1$. Another regular singularity may occur at some value of r in the range of $0 < r \leq 1$ for which $\gamma(r) = 0$ ($\gamma(0) = 0$ gives an irregular singularity at $r = 0$ and must be handled differently). For $\gamma(r) = 0$ in the range $0 < r \leq 1$, the integration path must be deformed in agreement with Lin's (ref. 22) criterion. The flows of interest (i.e., on which the group velocity C_g has a minimum value) in the present problem turn out to be outside the range $\gamma(r) = 0$ for $0 < r \leq 1$.

The dispersion relations and hence the group velocities for axisymmetric ($n = 0$) and asymmetric ($n = \pm 1$) waves have been obtained numerically for the mean profiles at each axial station considered as a parallel flow and are presented in the next section.

RESULTS AND DISCUSSION

In this section, the numerical results for the characteristics of wave propagation along the duct are presented. The velocity distribution in the duct is taken as the solution found by the inviscid quasi-cylindrical approximation. The analysis is applied at various axial stations along the divergent duct for $q = 0.8$, 1.0, 1.429, 1.667, and 2.0 (figs. 1-5).

The group velocities for the axisymmetric mode ($n = 0$) are shown in the figures 6 through 10. It can be seen that the group velocity for the flow region ahead of the stagnation point is directed downstream (i.e., $C_g > 0$ for

all wave number k) and hence the flow is supercritical ahead of the stagnation point, except for $q = 2.0$. For the region behind the stagnation point, the group velocity is directed upstream and hence the flow is subcritical behind the stagnation point. Recall that the flow downstream of the stagnation point is physically meaningless in that Γ is undefined for negative ψ. The wave propagation results are presented in this region of interest. The slope of the amplitude function of radial perturbation velocity near $r = 0$ becomes larger as its axial location approaches the stagnation point. This occurs when $\gamma_o = \omega + n(V/r)|_{r=0} + kW|_{r=0}$ goes to zero at $r = 0$ so that the Frobenius power series solution near $r = 0$ (obtained from the eq. (6)) becomes invalid.

Therefore, for the axisymmetric mode ($n = 0$) of wave propagation, near the stagnation point of the basic flow field, the approach to the irregular singularity $\gamma_o = 0$ causes the group velocity to go to zero. However, this observation is only qualitatively true since the parallel flow assumption is not valid near the stagnation point.

For the asymmetric mode ($n = 1$), the group velocities are presented in figures 11 through 15. Note that the group velocity generally decreases as the axial station moves downstream toward the stagnation point for supercritical flows, except when $q = 1.429$ (fig. 13). Once again, C_g may cross zero in the range $1.36 < R(z) < 1.43$ and $1.2 < R(z) < 1.33$ for $q = 0.8$ and 1.0, which is the region containing the stagnation point. If we check a typical amplitude function of the radial perturbation velocity (shown in figs. 16 and 17), we see that the slope of the amplitude functions for which C_g is minimum, is very large near $r = 0$ as its axial station approaches the stagnation point. This situation is similar to the axisymmetric case discussed previously. Figure 13 shows the group velocity at various axial stations for $q = 1.429$. It is seen that, at the inlet of the divergent duct, $C_{g_{min}}$ is very close to zero, but the amplitude function (fig. 18) of the radial perturbation velocity is well behaved. (Figure 19 shows the amplitude function at axial station behind the stagnation point.) As the station being studied moves downstream, $C_{g_{min}}$ does not cross zero, but increases as its axial station moves closer to the stagnation point. This result differs from the two cases for $q = 0.8$ and 1.0 discussed previously. For $q = 1.667$, the flow at the inlet of the duct is still supercritical to the axisymmetric waves (fig. 9), but is subcritical to the asymmetric ($n = 1$) waves (fig. 14). For $q = 2.0$ (which is only slightly larger than Benjamin's (ref. 11) critical value of 1.92), figures 10 and 15 show that the flow is subcritical to both axisymmetric and asymmetric waves. However, figure 10 shows that this flow is subcritical to a mode having the simple structure of the amplitude function, but is still supercritical to a different mode having several nodes along the radial axis in its amplitude function.

The group velocities of asymmetric mode ($n = -1$) at various axial stations for various q values are shown in figures 20 through 24. The flows are supercritical at the inlet of the duct except for $q = 2.0$. (Figure 24 shows that C_g at $R(z) = 1.0$ crosses zero in the long wavelength limit.)

The numerical results for phase velocities are presented in figures 25 through 38. The directions of group velocities and phase velocities and the states of the flows are compared in table 1. For $q \leq 1.667$ (which is less than q_c), the directions of group velocity and phase velocity are the same for modes $n = 0$ and 1 at the same axial locations. The exception is mode $n = 1$ for $q = 1.667$. For mode $n = -1$ of all cases, and modes $n = 0, \pm 1$ of case $q = 2.0$, the directions of the group velocity and phase velocity are not the same in a certain range of wave number k.

CONCLUSIONS

The linear wave propagation analysis has been applied to an idealized model of the flow in a slowly diverging duct having inlet conditions of solid-body rotation and uniform axial velocity. For a varying q (the ratio of swirl velocity to axial velocity at the inlet), the wave propagation of various modes at each axial station (treated as a parallel flow) has been calculated. Although the development of the flow field in the divergent duct described by the inviscid quasi-cylindrical approximation is unrealistic in the region near the downstream stagnation point, it may be of interest to identify the wave propagation characteristics of these different flow regions.

At the present stage, we conclude the following for this idealized flow model:

(a) If the critical state is defined as done by Benjamin (ref. 10), the flow that is supercritical cannot be driven to be subcritical simply by the divergent wall of the duct. However, if the critical state is defined by the group-velocity criterion $C_g = 0$, the flow that is supercritical can be driven to be subcritical due to the occurrence of the stagnation point by the divergent wall of the duct.

(b) As the stagnation point is approached, the group velocity C_g goes to zero for the axisymmetric waves. However, the parallel flow assumption near the stagnation point is not valid.

(c) The directions of phase velocity and group velocity are consistent only for modes $n = 0$ and 1 in the flow that is supercritical upstream of the stagnation point.

REFERENCES

1. Lebovich, S.: The Structure of Vortex Breakdown. Ann. Rev. Fluid Mech., vol. 10, 1978, p. 221.

2. Harvey, J. K.: Some Observations of the Vortex Breakdown Phenomenon. J. Fluid Mech., vol. 14, 1962, p. 585.

3. Sarpkaya, T.: On Stationary and Travelling Vortex Breakdowns. J. Fluid Mech., vol. 45, pt. 3, 1971, p. 545.

4. Faler, J. H.; and Lebovich, S.: Disrupted States of Vortex Flow and Vortex Breakdown. Physics of Fluids, vol. 20, no. 9, 1977.

5. Faler, J. H.; and Lebovich, S.: An Experimental Map of the Internal Structure of a Vortex Breakdown. J. Fluid Mech., vol. 86, pt. 2, 1978, p. 313.

6. Garg, A. K.: Oscillatory Behavior in Vortex Breakdown Flows: an Experimental Study Using a Laser Doppler Anemometer." M.S. Thesis, Cornell Univ., 1977.

7. Hall, M. G.: Vortex Breakdown. Ann. Rev. Fluid Mech., vol. 4, 1972, p. 195.

8. Ludweig, H.: Vortex Breakdown. Deutsche Luft-und Raumfahrt Rept. 70-40, 1970.

9. Squire, H. B.: Analysis of the Vortex Breakdown Phenomenon, Part I. Dept. of Aero. Rept. 102, Imperial College, London, 1960.

10. Benjamin, B. T.: Theory of the Vortex Breakdown Phenomenon. J. Fluid Mech., vol. 14, 1962, p. 593.

11. Randall, J. D.; and Lebovich, S.: The Critical State: a Trapped Wave Mode of Vortex Breakdown. J. Fluid Mech., vol. 53, 1973, p. 495.

12. Landahl, M. T.: Wave Mechanics of Breakdown. J. Fluid Mech., vol. 56, pt. 4, 1972, p. 775.

13. Bilanin, A. J.: Wave Mechanics of Line Vortices. Ph.D. Thesis, Massachusetts Institute of Technology, 1973.

14. Batchelor, G. K.: An Introduction to Fluid Dynamics. Cambridge University Press, 1967.

15. Thomson, Sir W.: Mathematical and Physical Papers, Vol. IV. Cambridge University Press, 1910.

16. Howard, L. N.; and Gupta, A. S.: On the Hydrodynamic and Hydromagnetic Stability of Swirling Flows. J. Fluid Mech., vol. 14, 1962, p. 463.

17. Pedley, T. J.: On the Instability of Rapidly Rotating Shear Flows to Nonaxisymmetric Disturbances." J. Fluid Mech., vol. 31, pt. 3, 1968, p. 603.

18. Uberoi, M. S.; Chow, C. Y.; and Narain, J. P.: Stability of Coaxial Rotating Jet and Vortex of Different Densities. Physics of Fluids, vol. 15, 1972, p. 1718.

19. Lessen, M.; Deshpande, N. Y.; and Hadji-Ohanes, B.: Stability of a Potential Vortex with Non-Rotating andRigid-Body Rotating Top-Hat Jet Core. J. Fluid Mech., vol. 60, 1973, p. 459.

20. Lessen, M.; Singh, P. J.; and Paillet, F.: The Stability of a Trailing Line Vortex, Pt. 1, Inviscid Theory. J. Fluid Mech., vol. 63, pt. 4, 1974, p. 753.

21. Hultgren, L.: Stability of Axisymmetric Gas Flows in a Rapidly Rotating Cylindrical Container. Ph.D. Thesis, Massachusetts Institute of Technology, 1978.

22. Lin, C. C.: The Theory of Hydrodynamic Stability. Cambridge University Press, 1955.

TABLE 1.- COMPARISON OF DIRECTIONS OF GROUP VELOCITY C_g AND PHASE VELOCITY C_p AND THE STATE OF THE FLOW CONDITION AHEAD OF THE STAGNATION POINT

q	Mode n = 0	Mode n = 1	Mode n = -1
0.8	Same Supercritical	Same Supercritical	Not the same Supercritical
1.0	Same Supercritical	Same Supercritical	Not the same Supercritical
1.429	Same Supercritical	Same Supercritical	Not the same Supercritical
1.667	Same Supercritical	Not the same Subcritical	Not the same Supercritical
2.0	Not the same Subcritical	Not the same Subcritical	Not the same Subcritical

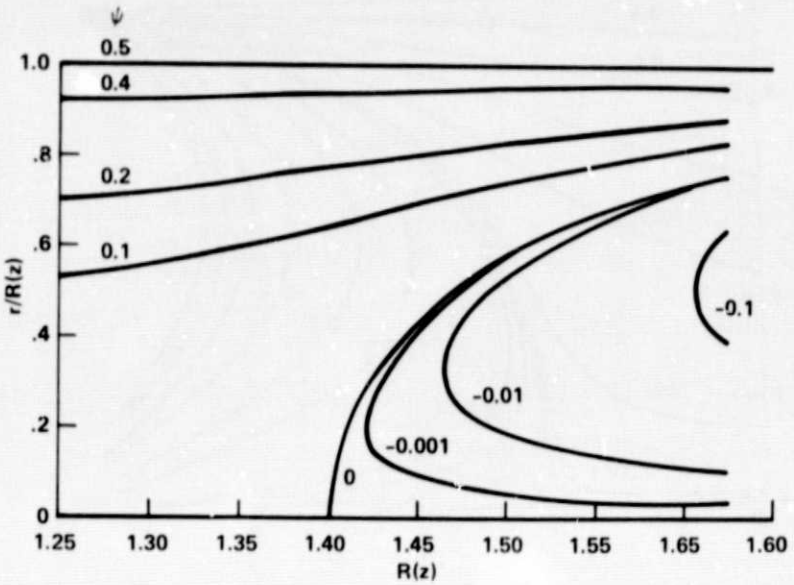

Figure 1.- Stream function in a divergent duct for q = 0.8.

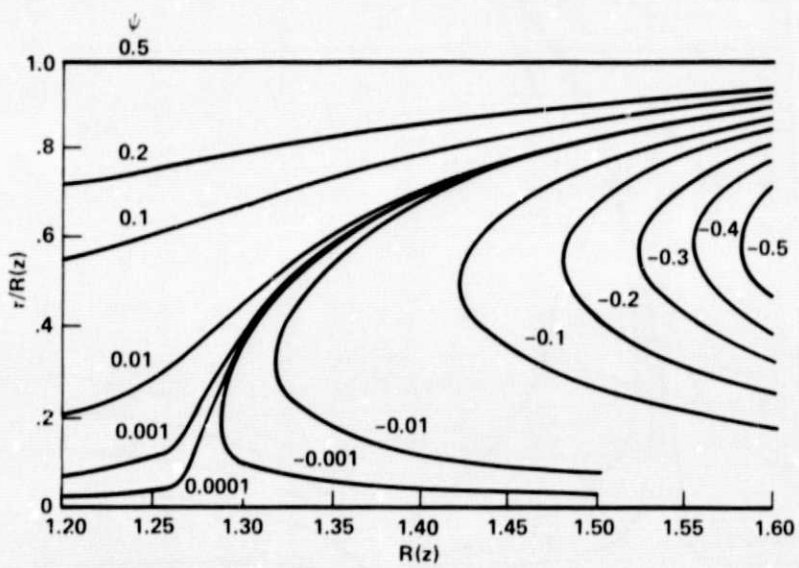

Figure 2.- Stream function in a divergent duct for q = 1.0.

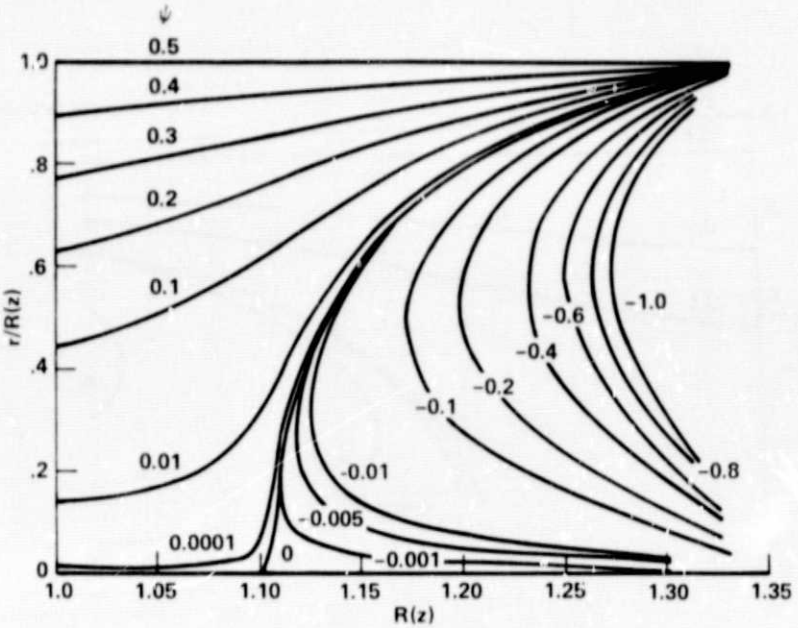

Figure 3.- Stream function in a divergent duct for q = 1.429.

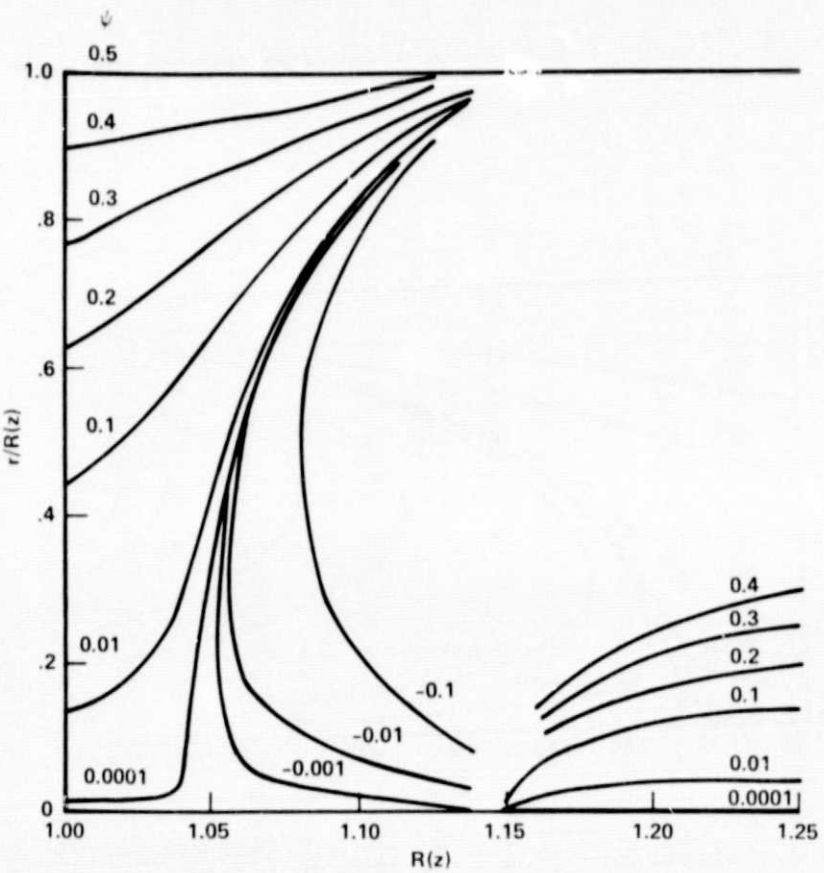

Figure 4.- Stream function in a divergent duct for q = 1.667.

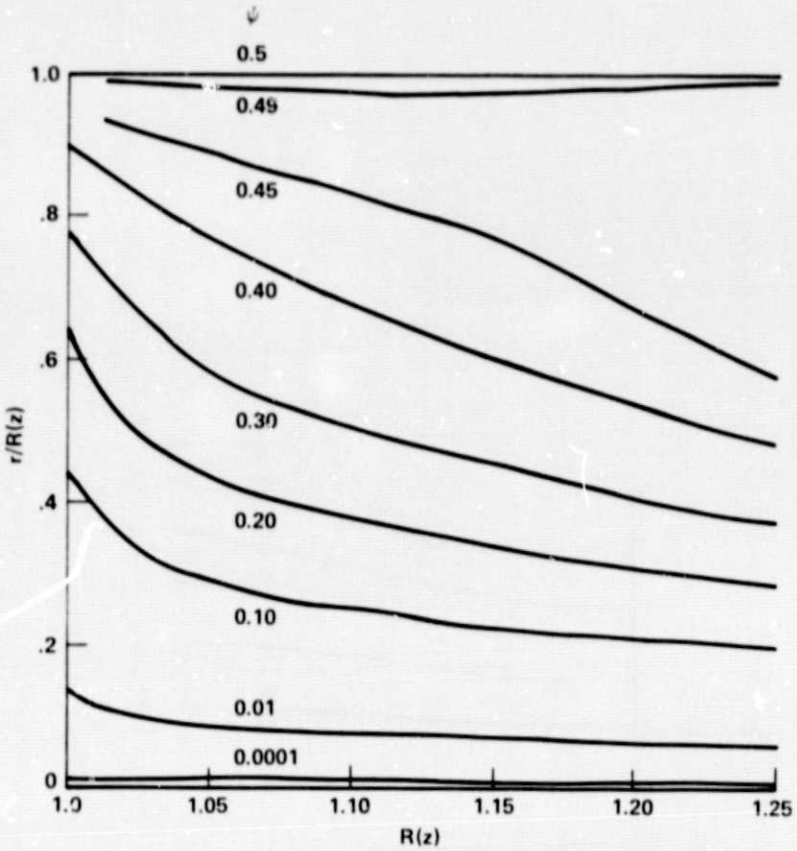

Figure 5.- Stream function in a divergent duct for q = 2.0.

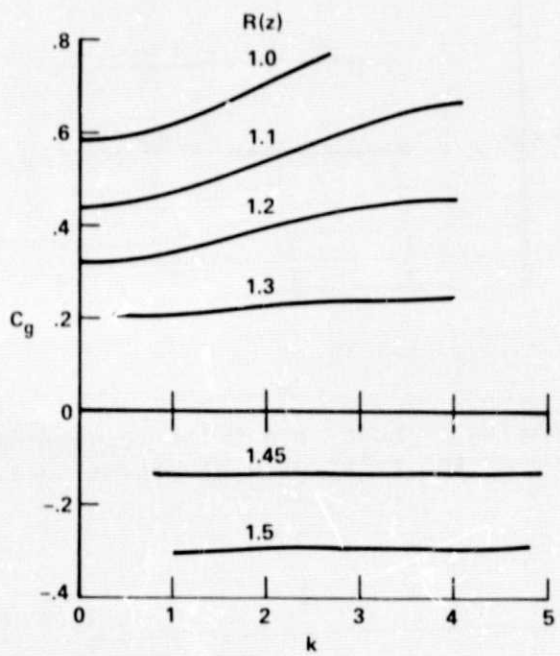

Figure 6.- Group velocities of mode n = 0 at various axial stations for q = 0.8 at the inlet of a divergent duct.

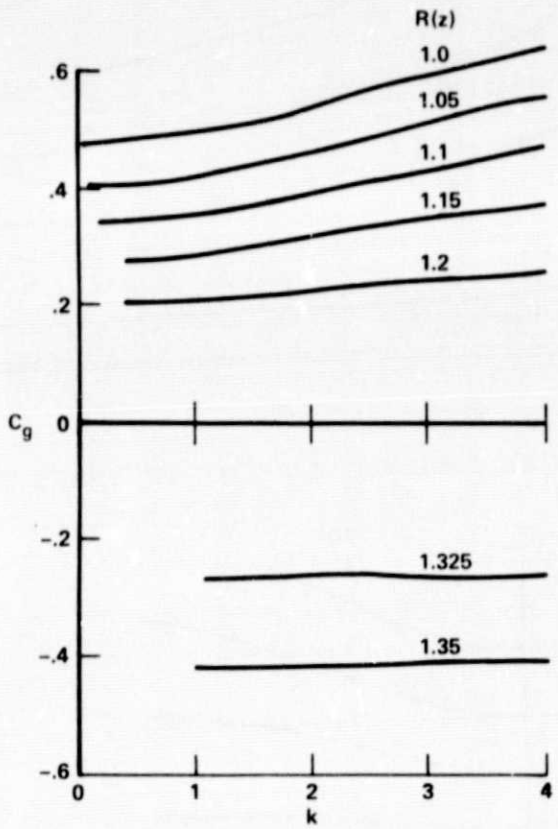

Figure 7.- Group velocities of mode n = 0 at various axial stations for q = 1.0 at the inlet of a divergent duct.

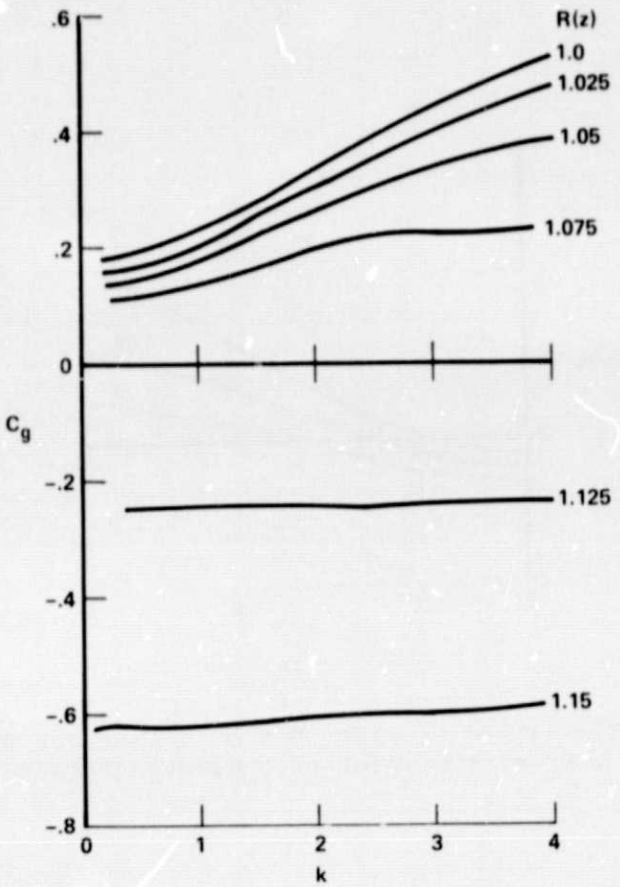

Figure 8.- Group velocities of mode n = 0 at various axial stations for q = 1.429 at the inlet of a divergent duct.

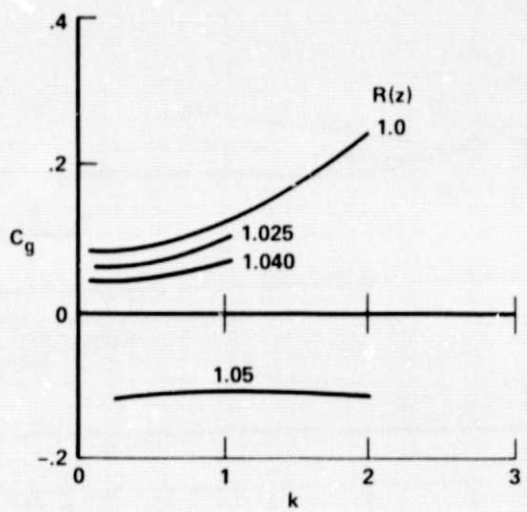

Figure 9.- Group velocities of mode n = 0 at various axial stations for q = 1.667 at the inlet of a divergent duct.

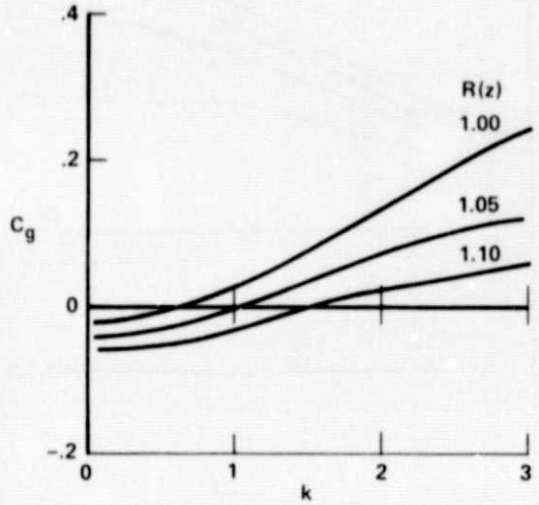

Figure 10.- Group velocities of mode n = 0 at various axial stations for q = 2.0 at the inlet of a divergent duct.

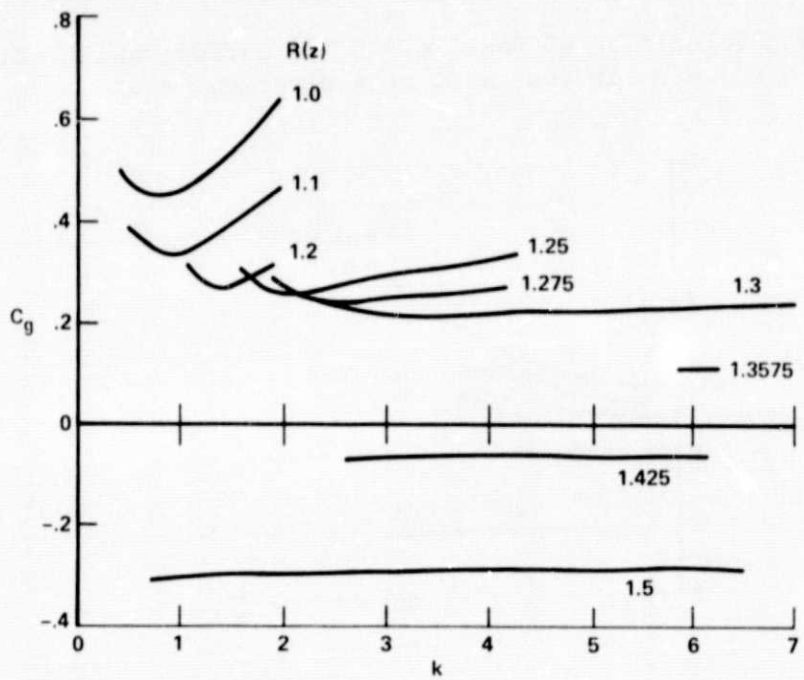

Figure 11.- Group velocities of mode n = 1 at various axial stations for q = 0.8 at the inlet of a divergent duct.

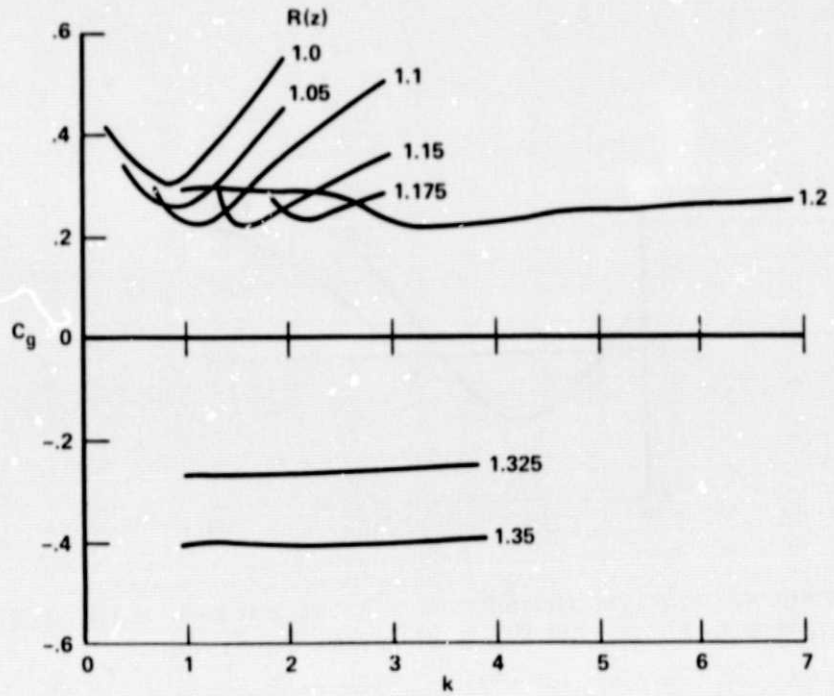

Figure 12.- Group velocities of mode n = 1 at various axial stations for q = 1.0 at the inlet of a divergent duct.

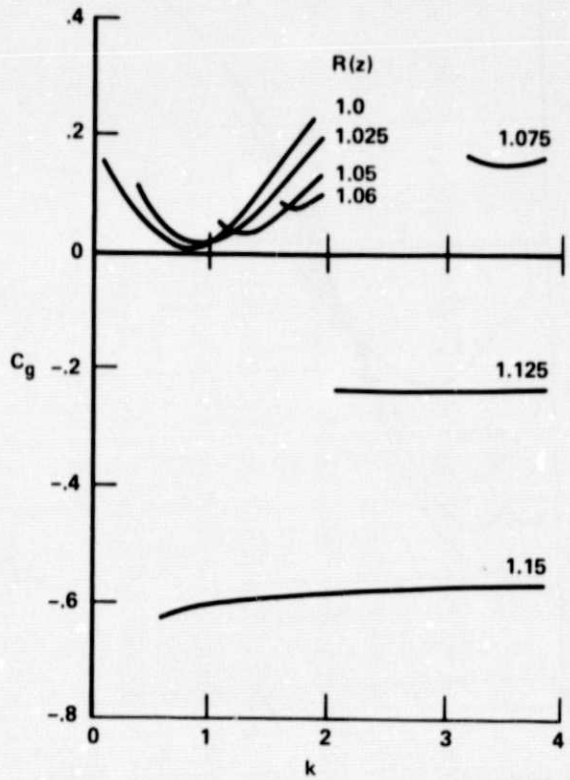

Figure 13.- Group velocities of mode n = 1 at various axial stations for q = 1.429 at the inlet of a divergent duct.

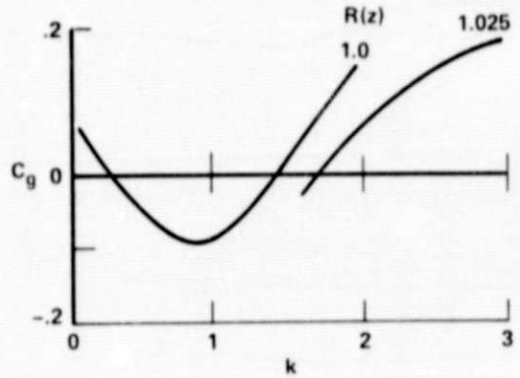

Figure 14.- Group velocities of mode n = 1 at various axial stations for q = 1.667 at the inlet of a divergent duct.

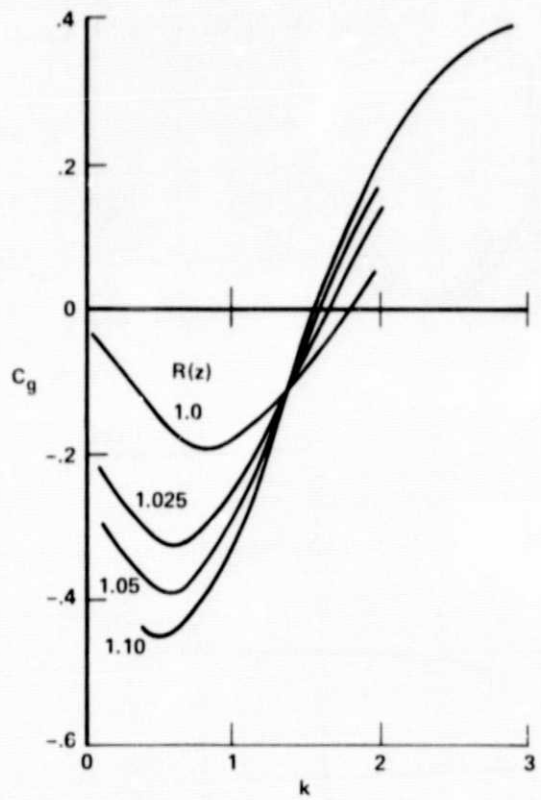

Figure 15.- Group velocities of mode n = 1 at various axial stations for q = 2.0 at the inlet of a divergent duct.

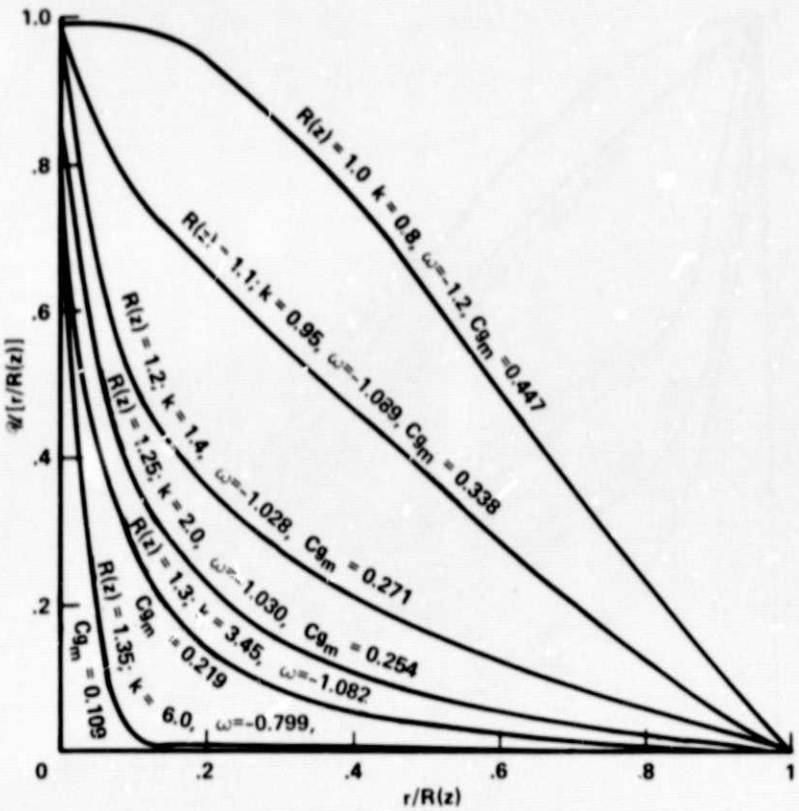

Figure 16.- Amplitude functions of radial perturbation velocities (mode n = 1) in a region ahead of the stagnation point for q = 0.8 at the inlet of a divergent duct.

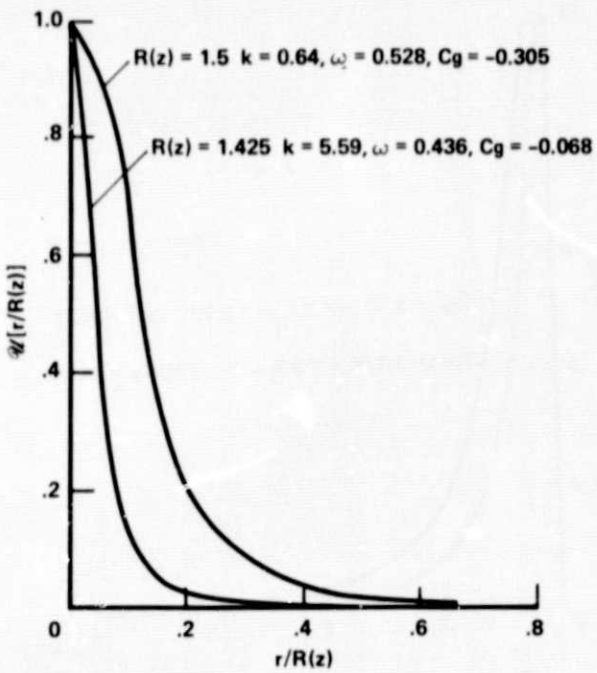

Figure 17.- Amplitude function of radial perturbation velocities (mode n = 1) in a region behind the stagnation point for q = 0.8 at the inlet of a divergent duct.

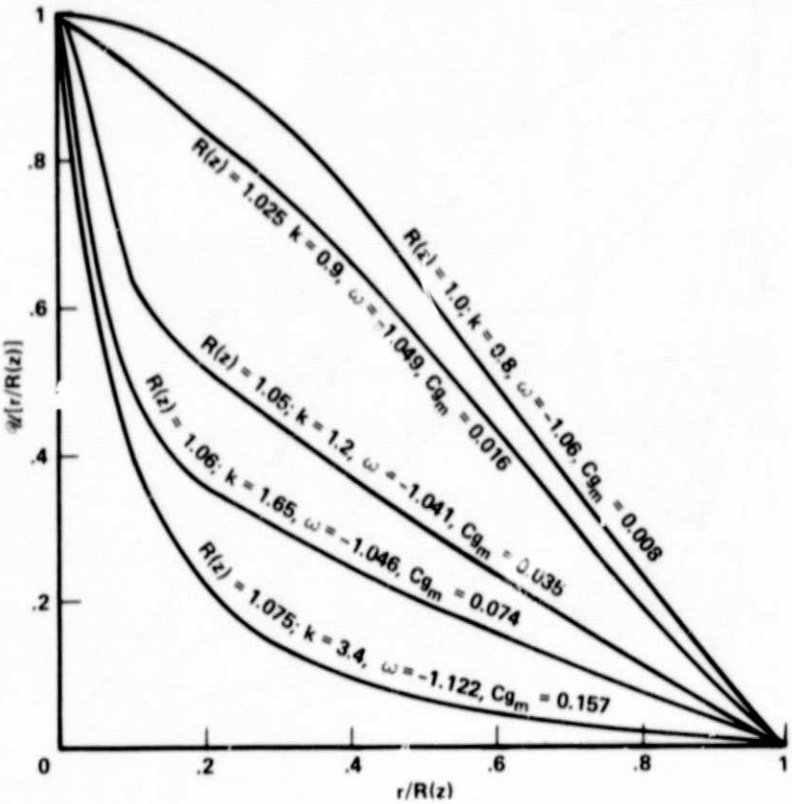

Figure 18.- Amplitude functions of radial perturbation velocities (mode n = 1) in a region ahead of the stagnation point for q = 1.429 at the inlet of a divergent duct.

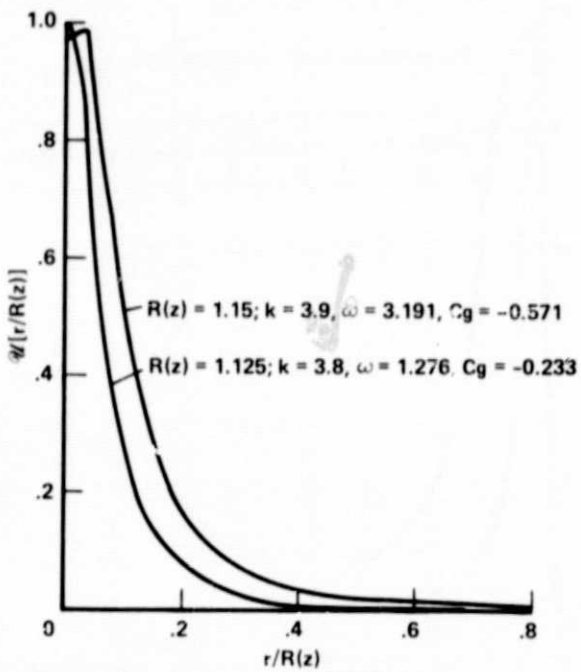

Figure 19.- Amplitude functions of radial perturbation velocities (mode n = 1) in a region behind the stagnation point for q = 1.429 at the inlet of a divergent duct.

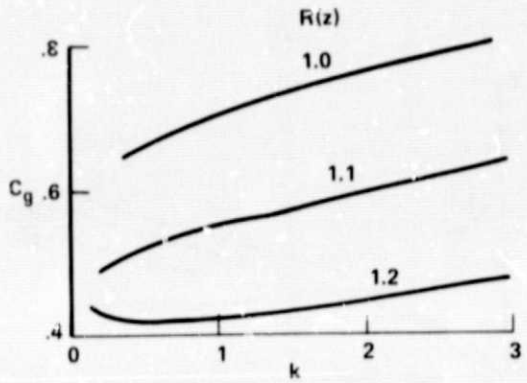

Figure 20.- Group velocities of mode n = -1 at various axial stations for q = 0.8 at the inlet of a divergent duct.

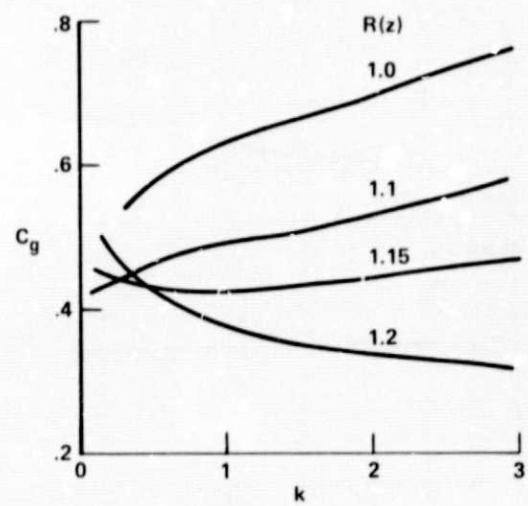

Figure 21.- Group velocities of mode n = -1 at various axial stations for q = 1.0 at the inlet of a divergent duct.

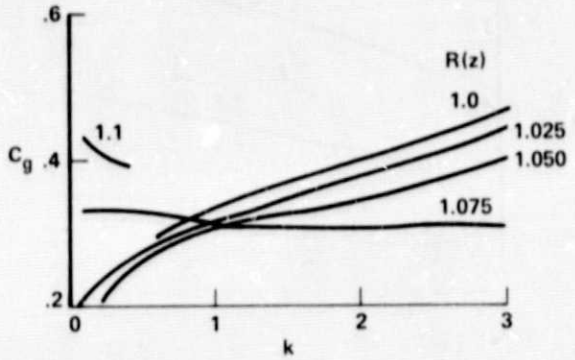

Figure 22.- Group velocities of mode n = -1 at various axial stations for q = 1.429 at the inlet of a divergent duct.

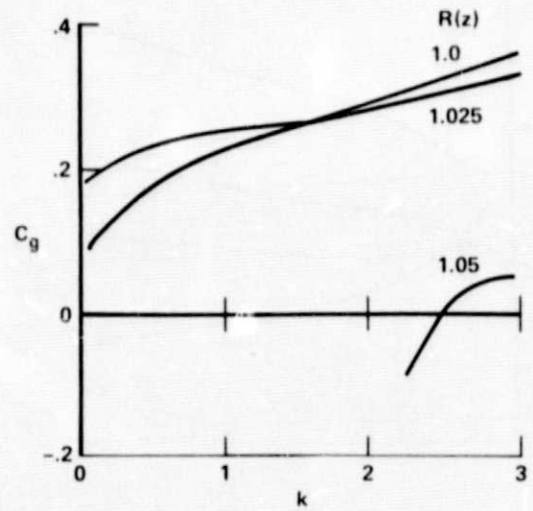

Figure 23.- Group velocities of mode n = -1 at various axial stations for q = 1.667 at the inlet of a divergent duct.

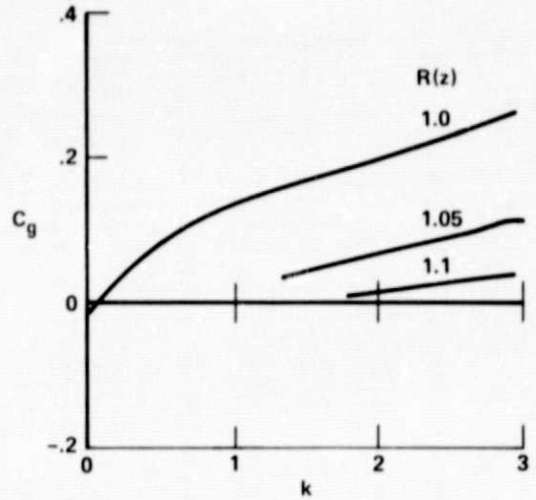

Figure 24.- Group velocities of mode n = -1 at various axial stations for q = 2.0 at the inlet of a divergent duct.

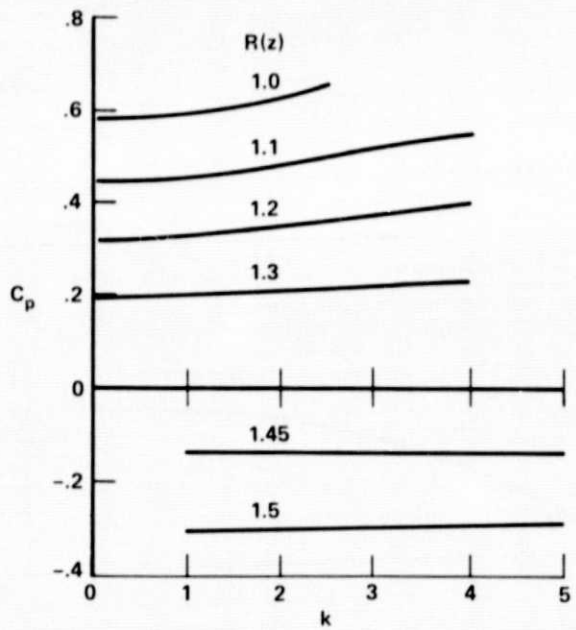

Figure 25.- Phase velocities of mode n = 0 at various axial stations for q = 0.8 at the inlet of a divergent duct.

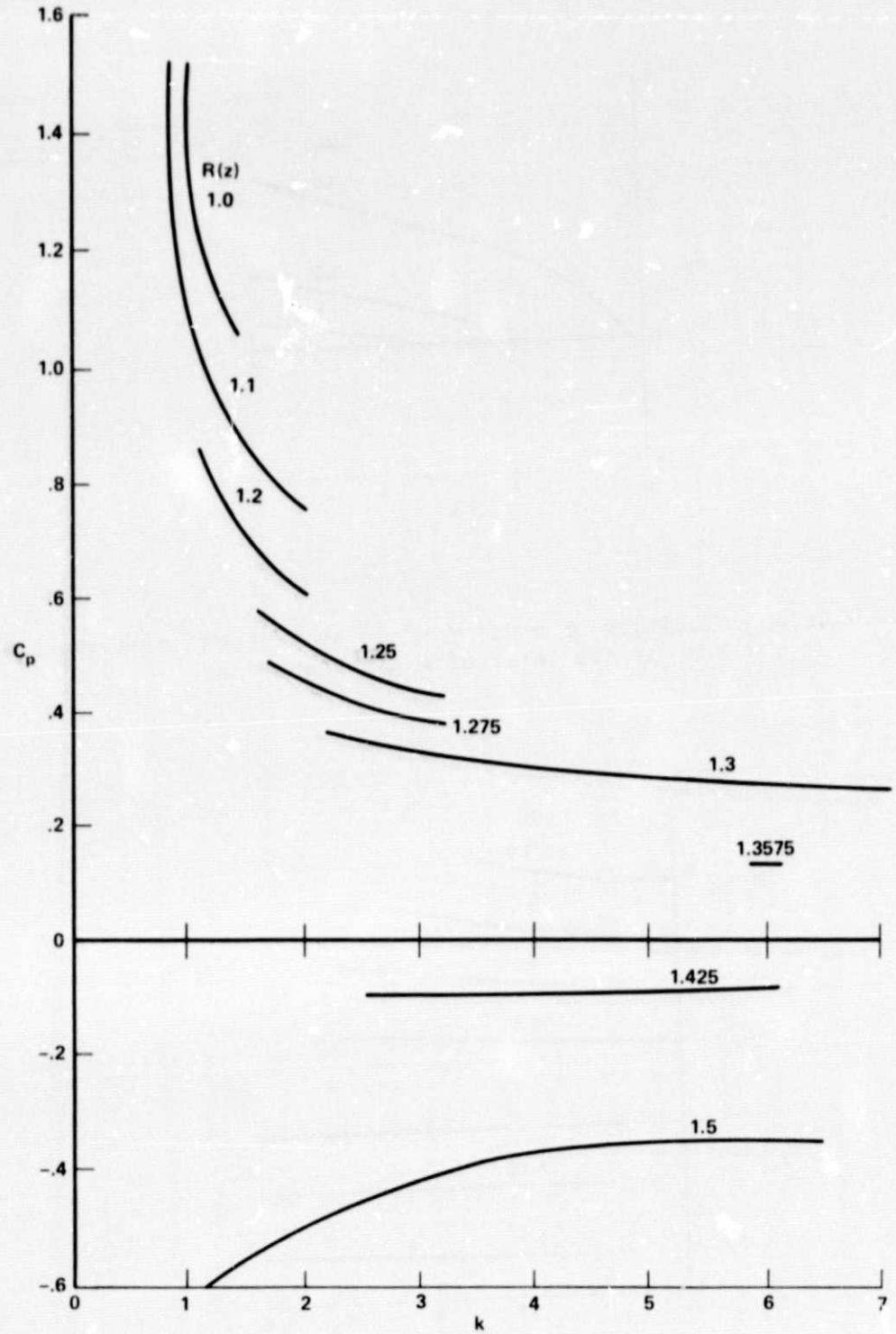

Figure 26.- Phase velocities of mode n = 1 at various axial stations for q = 0.8 at the inlet of a divergent duct.

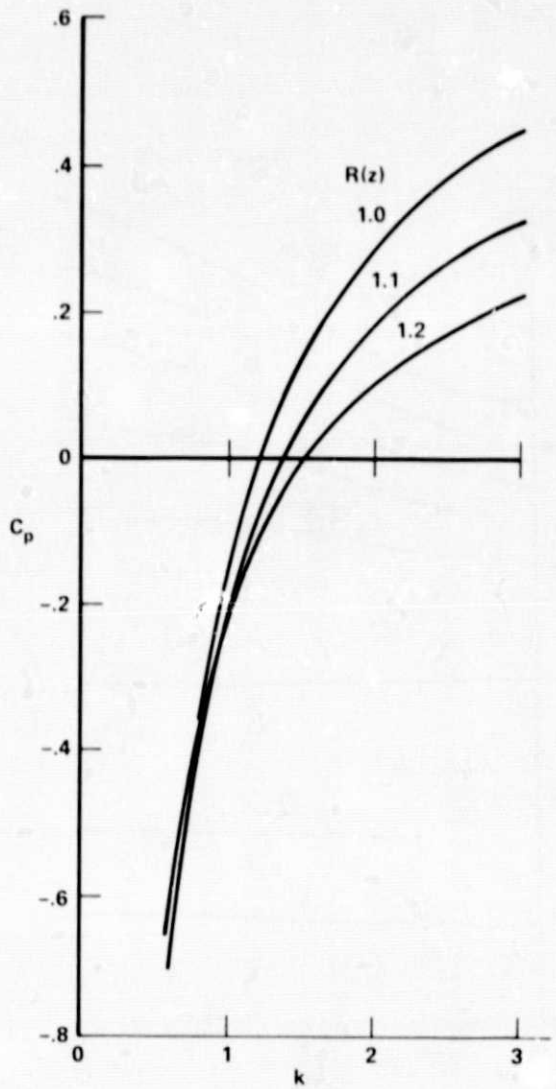

Figure 27.- Phase velocities of mode n = -1 at the various axial stations for q = 0.8 at the inlet of a divergent duct.

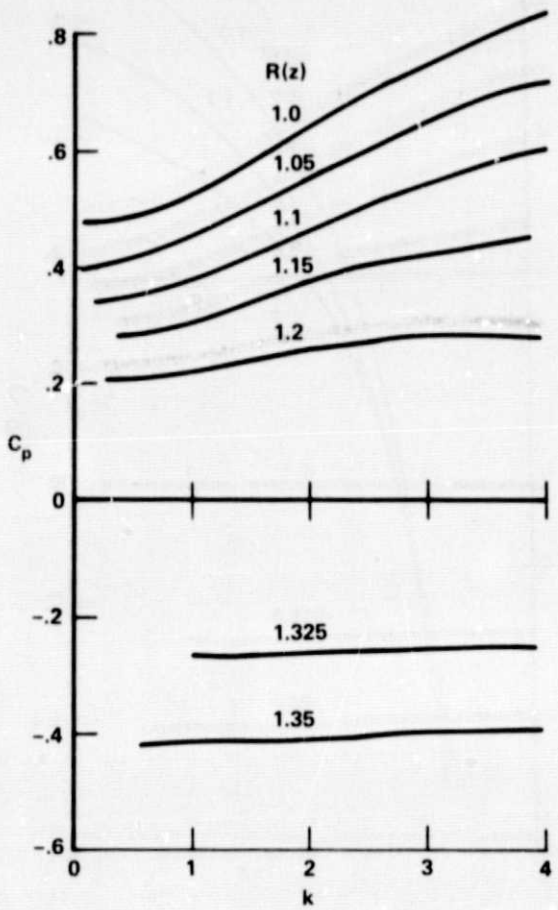

Figure 28.- Phase velocities of mode n = 0 at various axial stations for q = 1.0 at the inlet of a divergent duct.

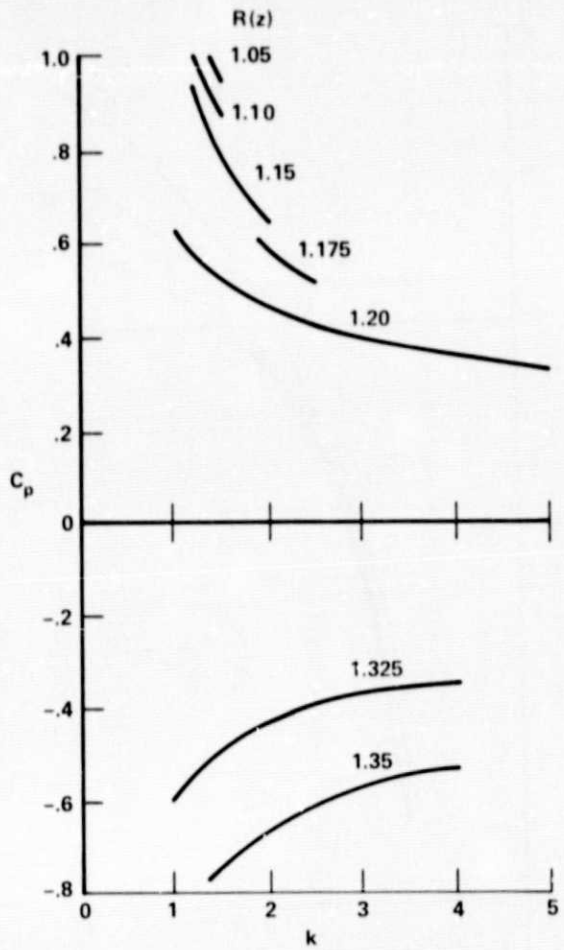

Figure 29.- Phase velocities of mode n = 1 at various axial stations for q = 1.0 at the inlet of a divergent duct.

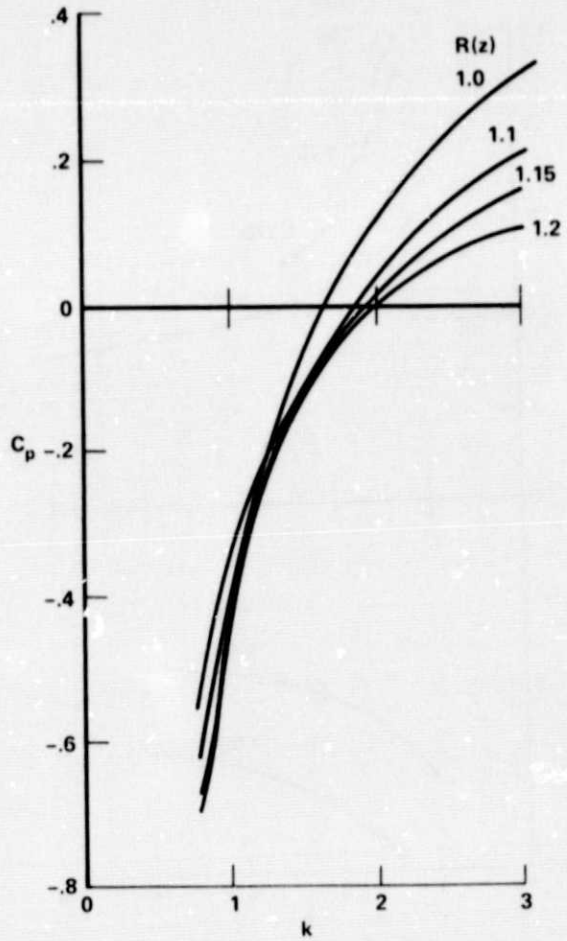

Figure 30.- Phase velocities of mode n = -1 at various axial stations for q = 1.0 at the inlet of a divergent duct.

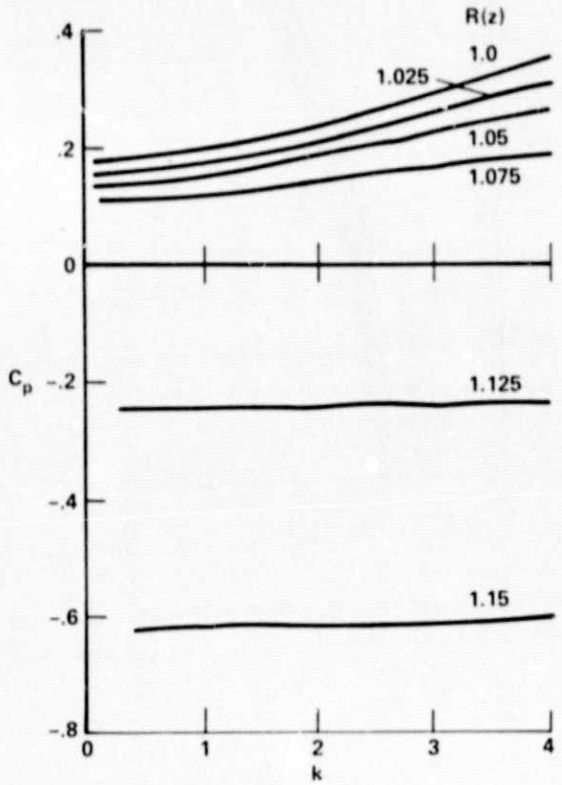

Figure 31.- Phase velocities of mode n = 0 at various axial stations for q = 1.429 at the inlet of a divergent duct.

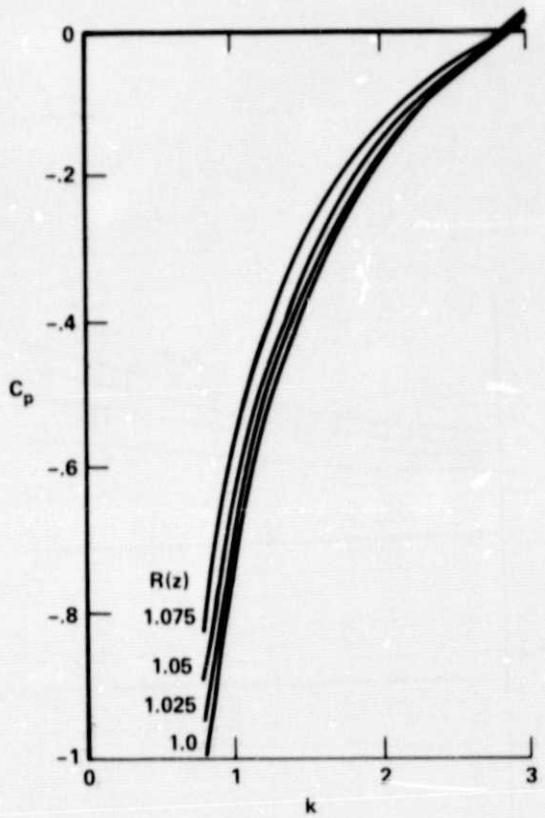

Figure 32.- Phase velocities of mode n = -1 at various axial stations for q = 1.429 at the inlet of a divergent duct.

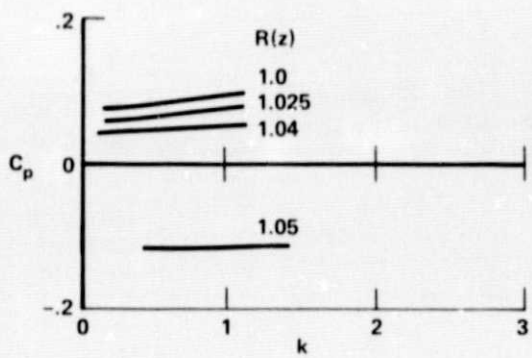

Figure 33.- Phase velocities of mode n = 0 at various axial stations for q = 1.667 at the inlet of a divergent duct.

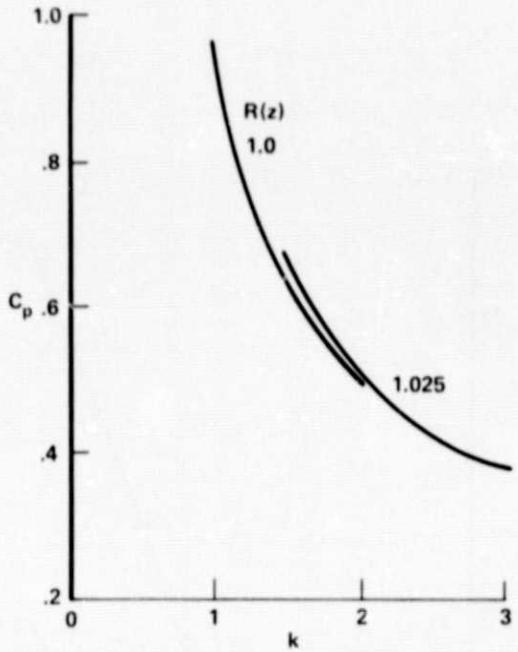

Figure 34.- Phase velocities of mode n = 1 at various axial stations for q = 1.667 at the inlet of a divergent duct.

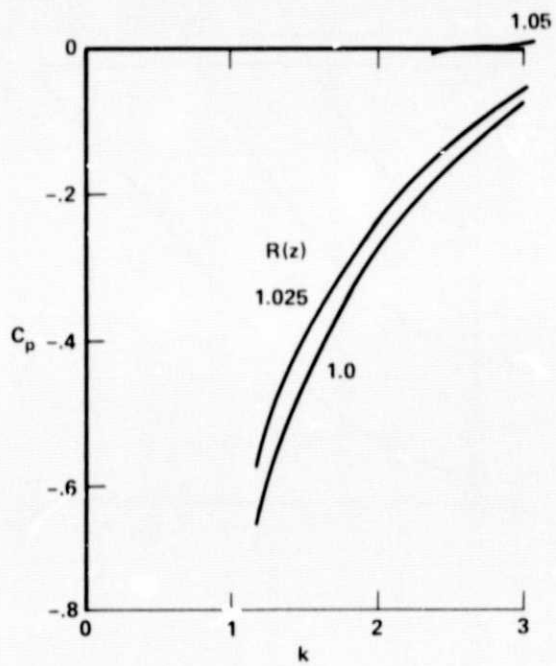

Figure 35.- Phase velocities of mode n = -1 at various axial stations for q = 1.667 at the inlet of a divergent duct.

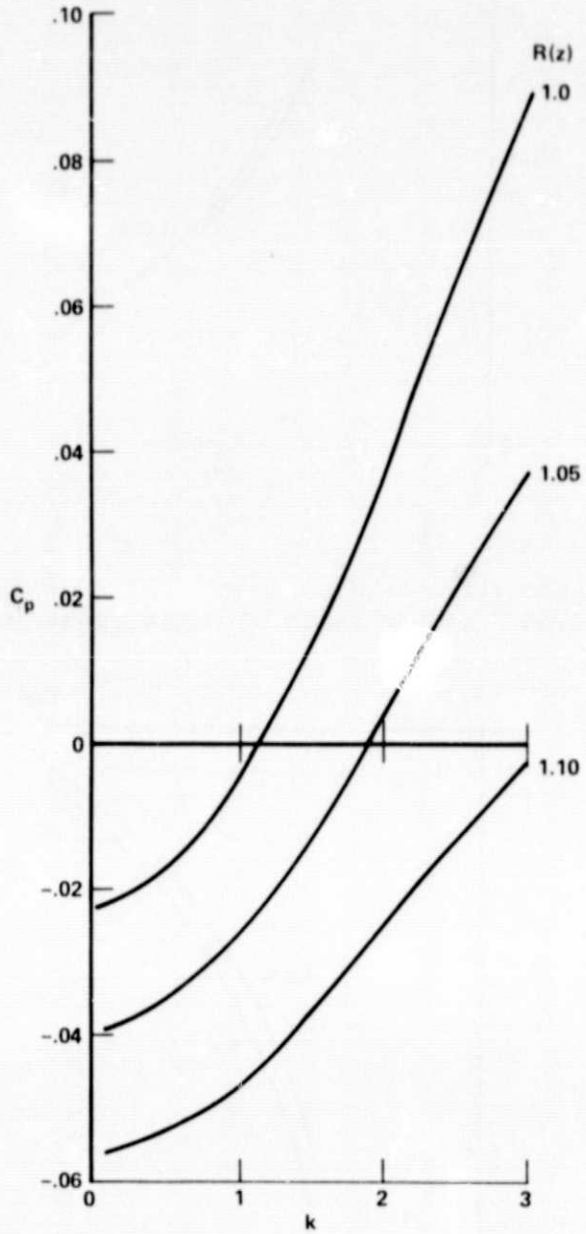

Figure 36.- Phase velocities of mode n = 0 at various axial stations for q = 2.0 at the inlet of a divergent duct.

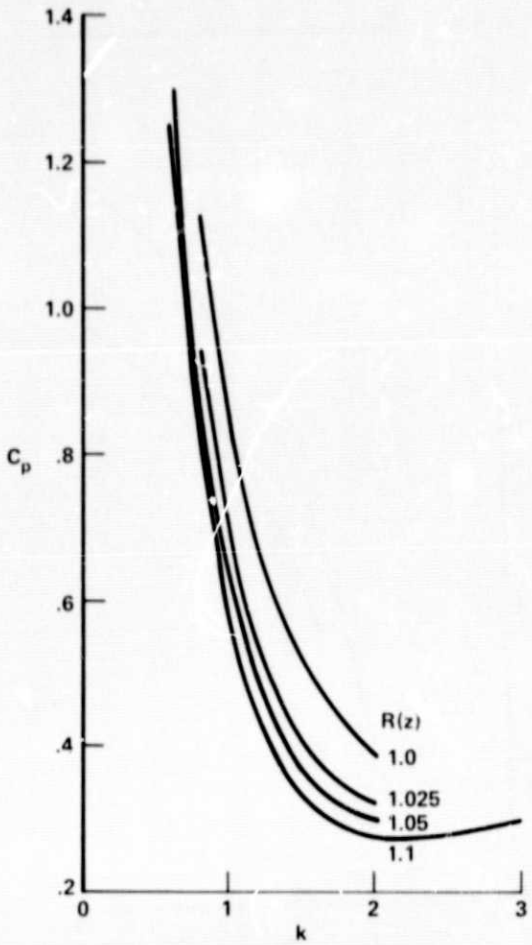

Figure 37.- Phase velocities of mode n = 1 at various axial stations for q = 2.0 at the inlet of a divergent duct.

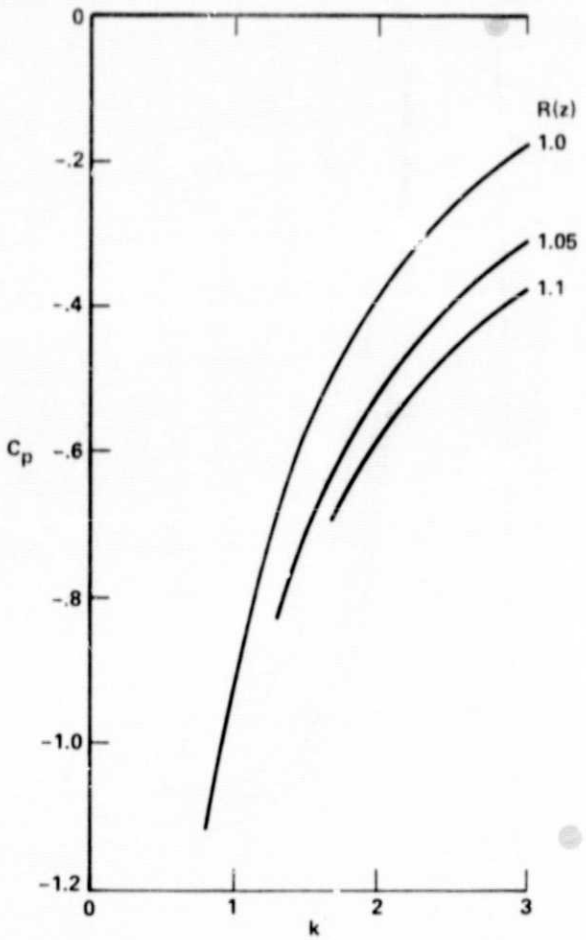

Figure 38.- Phase velocities of mode n = -1 at various axial stations for q = 2.0 at the inlet of a divergent duct.